The role of glass crystallization processes in preparation of high Li-conductive NASICON-type ceramics

Victor A. Vizgalov,[a] Tina Nestler,[b] Anastasia Vyalikh,[b] Ivan A. Bobrikov,[c] Oleksandr I. Ivankov,[c] Victor Petrenko,[c] Mikhail V. Avdeev,[c] Lada V. Yashina,[a] Daniil M. Itkis[a]

[a] Lomonosov Moscow State University, Leninskie gory 1, 119991 Moscow, Russian Federation.

[b] Technische Universität Bergakademie Freiberg, Leipziger Str. 23, D-09599 Freiberg, Germany.

[c] Joint Institute for Nuclear Research, Joliot-Curie 6,141980 Dubna, Russian Federation

Supporting information

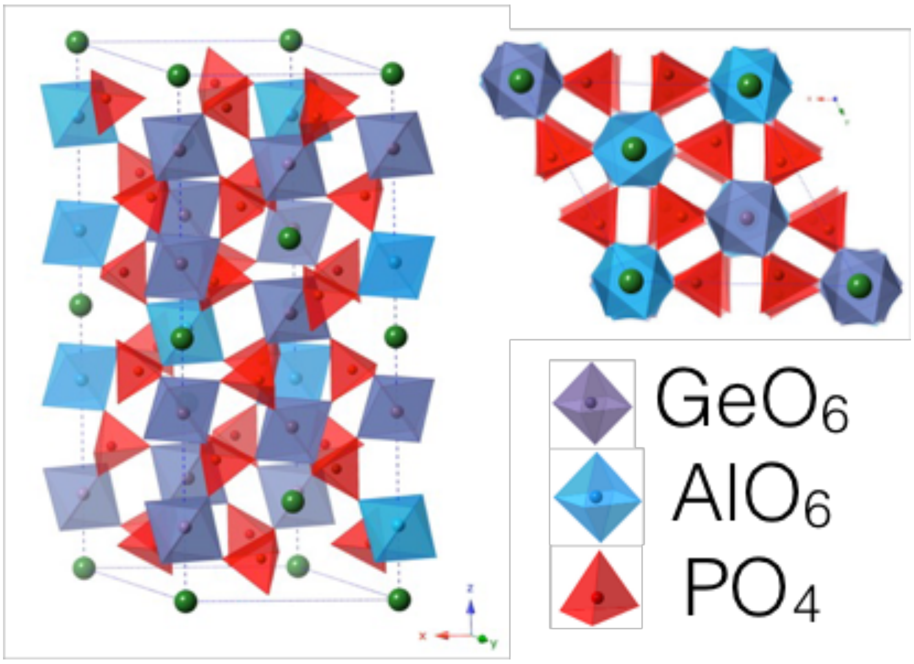

Figure S1. LAGP NASICON crystal structure. Red tetrahedra – PO4, Blue –. Figure S8 illustrates pathways between lithium positions –Li1-Li3-Li1–.

The term “NASICON” refers to the class of crystal structures that can be described as following: the crystal structure is built up by XO_4 tetrahedra, which share each corner oxygen atoms with BO_6 octahedra. Such framework contains a network of interconnected voids where Li^+ cations can move. Partial heterovalent substitution of B^{4+} cations by A^{3+} allows control of Li^+ content (x in $Li_{1+x}A_xB_{2-x}X_3O_{12}$) and, thus, enhancement of ionic conductivity due to occupation of Li sites in 3D tunnels of NASICON structure. Multicomponent glass system that is studied in this work crystallizes into NASICON structure. As mentioned above Li ions are distributed within channels available within PO_4, GeO_6 and AlO_6 polyhedral framework. In this channels two distinctive positions are recognized due to different sets of polyhedra surrounding this positions. They are generally referred to as Li1 and Li3 since in a number of papers it has been reported that at low temperature distinctive intermediate Li2 position can be observed.

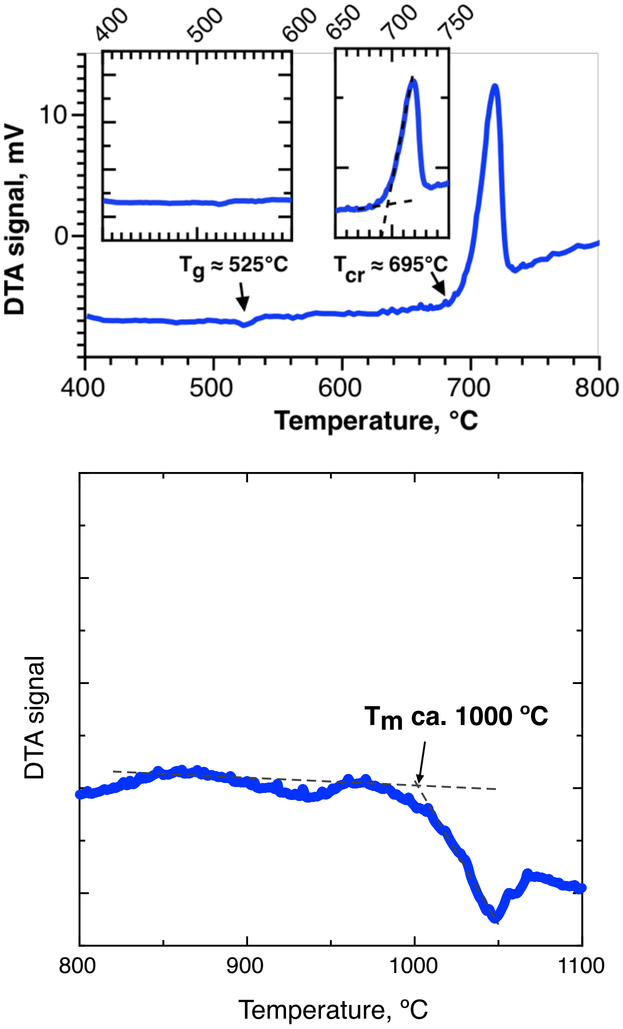

Figure S2. DTA data for glass Li_2O-Al_2O_3-GeO_2-P_2O_5 + Y_2O_3. Top plot represents T_g and T_c region, embedded plots more closely show corresponding temperature; bottom plot represents T_m region.

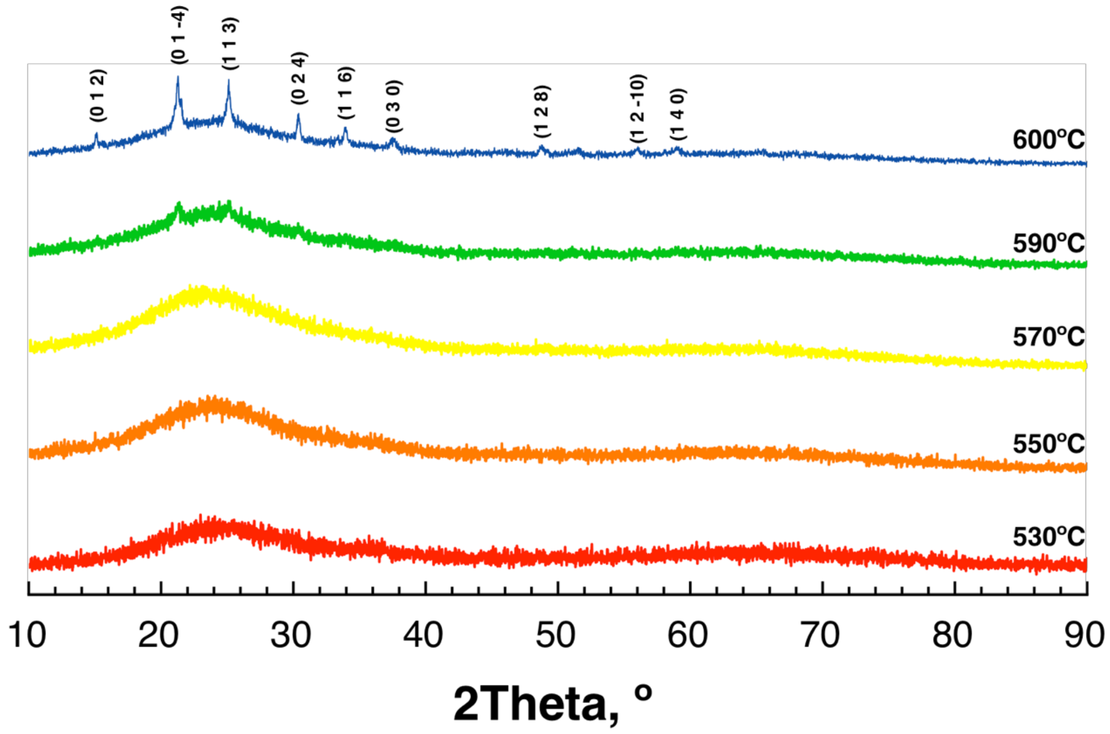

Figure S3. XRD patterns corresponding to glasses annealed at different temperatures for 30 minutes in order to optimize first annealing step conditions. Temperature range starts from 530ºC (slightly lower than glass vitrification point) up to 600ºC where first signs of crystallization appear.

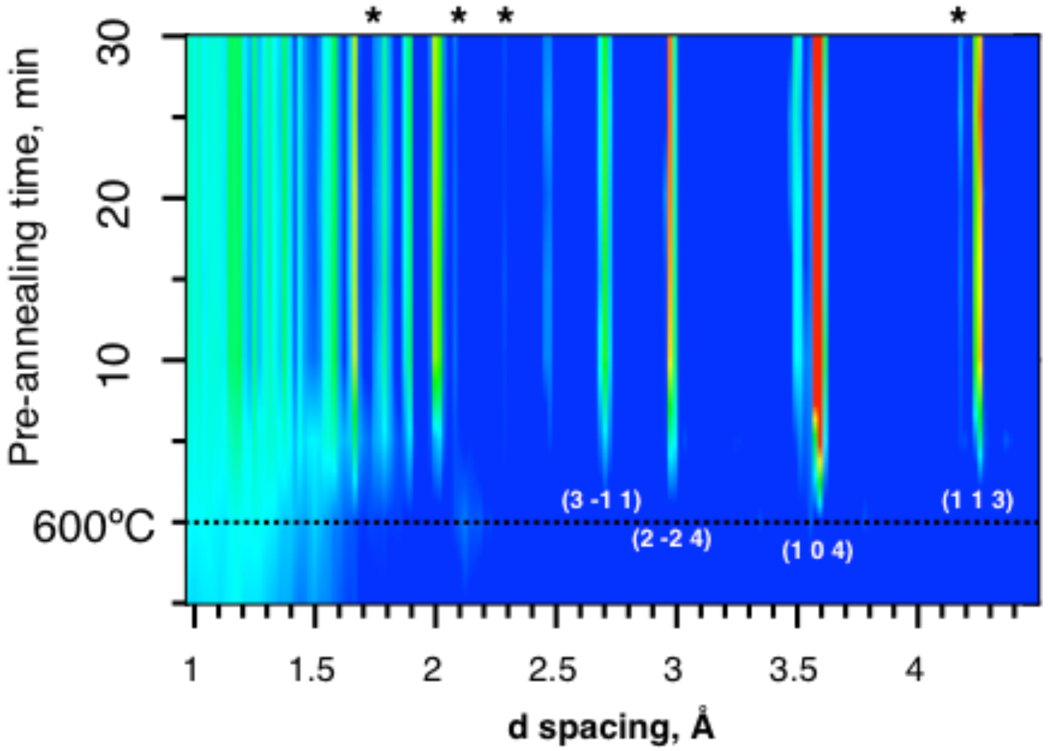

Figure S4. In situ neutron diffraction experiment during $Li_{1.5}Al_{0.5}Ge_{1.5}(PO_4)_3+Y_2O_3$ glass crystallization.

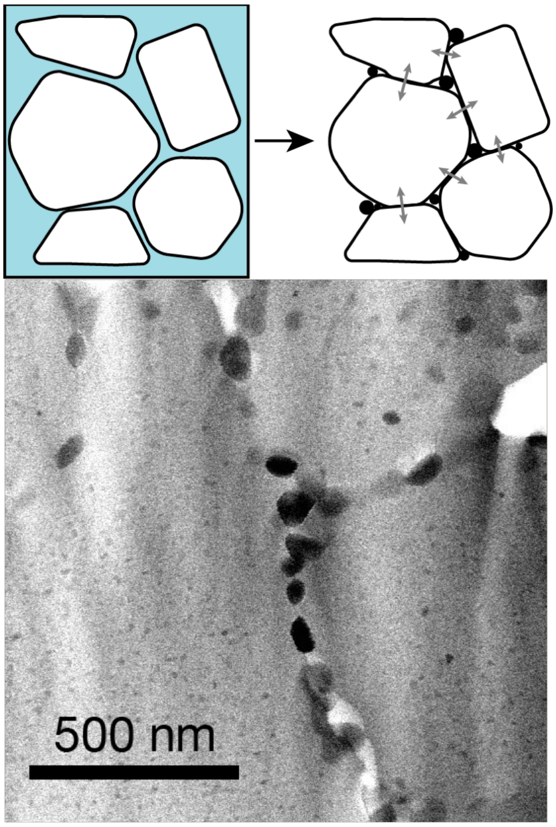

Figure S5. YPO_4 beads. Grey arrows show possible ionic conductivity paths.

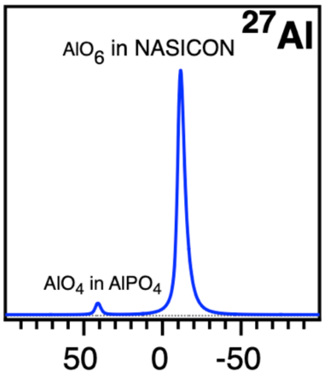

Figure S6. ^{27}Al NMR of glass-ceramic solid electrolyte, crystallized at 600ºC for 30min and at 750ºC for 2h

Conductivity estimation from structural and bond valence data

To clarify the origin of the Li-conductivity enhancement, the influence of the structural change of the unit cell on the conductivity is estimated by utilizing bond valence data. For the conductivity estimation based on the BVSE and obtained structural data it is stated that the charge carrier concentration is constant and no vacancies have to be generated for Li transport in the first place.

Assuming random walk diffusion, the tracer or self-diffusion coefficient D^* of the mobile Li ions can be calculated by

$$D^* \approx < r^2 > \nu e^{-\frac{E_{mig}}{k_B T}}, \text{ Eq. 1}$$

where r is the jump distance between Li1 sites, E_{mig} the migration barrier calculated by the bond valence site energy method, k_B being the Boltzmann constant and T the absolute temperature. The hopping attempt frequency ν is estimated to be 10^{12} Hz [1]. The diffusivity connects to the measurable conductivity via the Nernst-Einstein/Einstein-Smoluchowski relation

$$\sigma = \frac{D^* H_R c Q^2}{k_B T}, \text{ Eq. 2}$$

with c denoting the charge carrier concentration (Li on the Li1 sites), H_r the Haven ratio, which is close to 1, and Q being the charge of the conducting ion (1).

Migration Path according to BVSE calculations

According to the BVSE calculations, the Li on the Li1 site is mobile, as six symmetrical equivalent curved paths lead to the neighboring Li1 sites. The intermediate position in this connecting path (black spheres, Fig. S8) are four-fold, nearly planarly, coordinated.

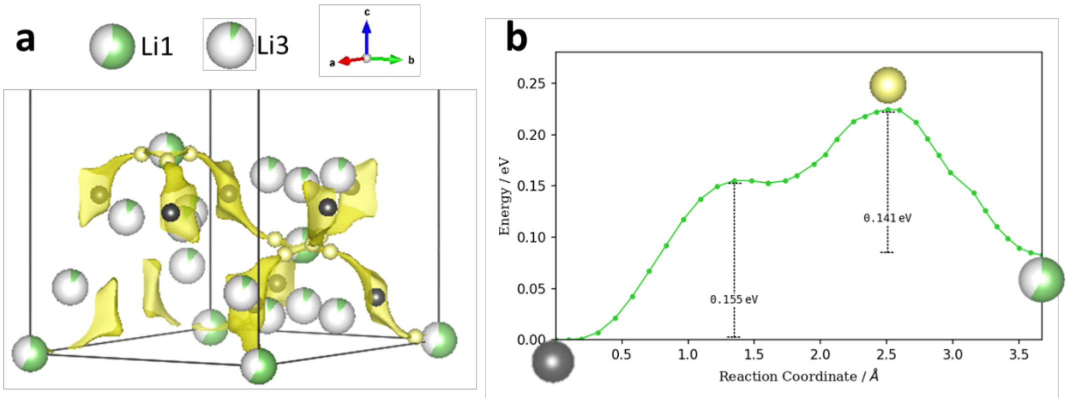

Figure S7. BVSE calculations for LAGPY at different annealing times by means of the structure data refined from neutron diffraction measurements: (a) Topology of the 3D migration path drawn with program VESTA [2], which allows illustrating the potential migration paths by marking areas with small BVSEs up to the calculated migration barrier. (b) The bottle neck and intermediate position in the path are marked by yellow and black spheres, respectively.

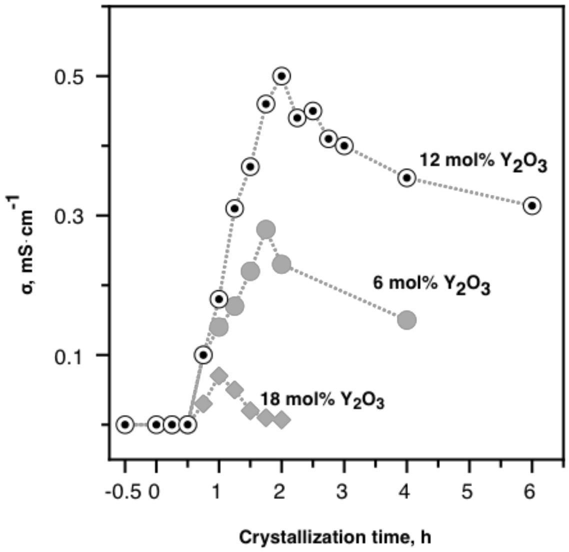

Figure S8. Ionic conductivity vs glass crystallization time for glass-ceramic with different concentration of Y_2O_3 added to the melts.

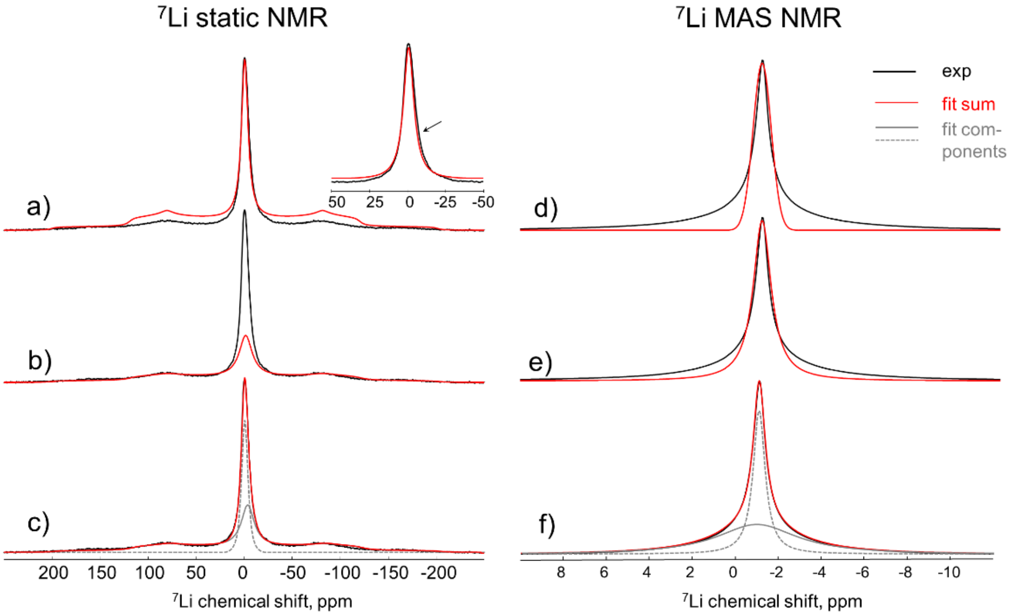

Figure S9. Fit (red line) of the 7Li static (left panel) and MAS (right panel) NMR spectra of LAGPY (black line) with a single fit component (a, b, d and e) showing a dismatch of the experimental and simulated spectra. The arrow on an inset in Fig. S1a points to a deviation of the right wing of the fit from the experimental spectrum provided that the quadrupole singularities at +/-100 ppm and a signal centrum (at ca. 0 ppm) coincide. Fit spectrum in d) is represented by a pure Gaussian function, and in e) by a pure Lorentzian function. Fitting with two components (grey lines) in c) and f) Their sum (red line) shows a very good agreement with the experimental spectra.

Bibliography

[1] Z. Rong, R. Malik, P. Canepa, G. Sai Gautam, M. Liu, A. Jain, K. Persson, G. Ceder, Chem. Mater. 27 (2015) 6016–6021.

[2] K. Momma, F. Izumi, Journal of Applied Crystallography 44 (2011) 1272–1276.